PROBING DENSE MATTER WITH STRANGE HADRONS

JOHANN RAFELSKI

Department of Physics, University of Arizona, Tucson, AZ 85721
and
CERN-Theory Division, 1211 Geneva 23, Switzerland

JEAN LETESSIER

Laboratoire de Physique Théorique et Hautes Energies
Université Paris 7, 2 place Jussieu, F–75251 Cedex 05.

Analysis of hadron production experimental data allows to understand the properties of the dense matter fireball produced in relativistic heavy ion collisions. We interpret the analysis results and argue that color deconfined state has been formed at highest CERN–SPS energies and at BNL–RHIC.

1   Quark-Gluon Plasma Phase Boundary

The signature of quark-gluon plasma is hard to identify, since the final state observed in the laboratory always consists of the same particles, irrespective of the transitional presence of the deconfined state. What changes is the detailed composition of the observed produced particle abundance. We consider here strangeness [1], and the pattern of strange hadron production at SPS and RHIC which offer, as we shall see, a compelling evidence for quark-gluon plasma formation.

An expanding fireball of quark and gluons breaks up into final state hadrons in conditions which differ from the equilibrium transformation explored in lattice QCD [2]. To understand this behavior we need to understand the pressure of quark-gluon plasma:

$$P_{\rm QGP} + \mathcal{B} = \frac{8c_1}{45\pi^2}(\pi T)^4 + \frac{n_{\rm f}}{15\pi^2}\left[\frac{7}{4}c_2(\pi T)^4 + \frac{15}{2}c_3\left(\mu_{\rm q}^2(\pi T)^2 + \frac{1}{2}\mu_{\rm q}^4\right)\right]. \quad (1)$$

We have inserted here the appropriate quark (with $n_{\rm f} = 2$) and gluon degeneracy. The interactions between quarks and gluons manifest their presence aside of the vacuum structure effect $\mathcal{B}$, in the three coefficients $c_i \neq 1$, see [3]:

$$c_1 = 1 - \frac{15\alpha_s}{4\pi} + \cdots, \quad c_2 = 1 - \frac{50\alpha_s}{21\pi} + \cdots, \quad c_3 = 1 - \frac{2\alpha_s}{\pi} + \cdots. \quad (2)$$

While higher order terms in the perturbative expansion have been obtained, they suggest lack of convergence of the expansion scheme formulated today. To reproduce the lattice results, near to $T = T_{\rm c}$, the bag constant, $\mathcal{B} = 0.19\,{\rm GeV/fm}^3$, is used.

The condition $P = P_{\rm p} - \mathcal{B} \to 0$, including the effect of motion reads [4],

$$\mathcal{B} = P_{\rm p} + (P_{\rm p} + \epsilon_{\rm p})\frac{\kappa v_{\rm c}^2}{1 - v_{\rm c}^2}, \qquad \kappa = \frac{(\vec{v}_{\rm c} \cdot \vec{n})^2}{v_{\rm c}^2}, \tag{3}$$

where subscript p refers to particle pressure and energy, and where we introduced the geometric factor κ which characterizes the angular relation between the surface normal vector and flow direction. The motion of quarks and gluons exercises additional pressure and thus the QGP phase remains the matter phase even below the static equilibrium transition temperature.

A fireball surface region which reaches condition Eq. (3) and continues to flow outwards must be torn apart. This is a collective instability and the ensuing disintegration of the fireball matter should be very rapid. A rapidly evolving fireball which supercools is in general highly unstable, and we expect that a sudden transformation (hadronization) into confined matter can ensue in such a condition. The situation we described could only arise since the vacuum pressure term is not subject to flow and always keeps the same value. An exploding QGP fireball only contained by the vacuum supercools to $T \simeq 145$ MeV. Hadrons are produced well below the equilibrium transition temperature $T \simeq 160$–170 MeV.

2 Statistical Hadronization

An extra reaction step 'hadronization' is required to connect the properties of the deconfined quark–gluon matter fireball, and the experimental apparatus. In this process, the quark and gluon content of the fireball is transferred into ultimately free flowing hadronic particles. In hadronization, gluons fragment into quarks, and quarks coalesce into hadrons. Color 'freezes', quark–gluon plasma excess entropy has to find a way to get away, so any additional production is hindered. It is far from obvious that hadron phase space (so called 'hadronic gas') be used consistently to describe the physics of thermal hadronization, and we establish now the consistency criterion assuming that entropy production is small, or even null, in hadronization of entropy rich thermal QGP into entropy poor hadron phases space.

Using the Gibbs–Duham relation for a unit volume, $\epsilon + P = T\sigma + \mu\nu$, the instability condition of dynamical expansion, Eq. (3), takes the form:

$$-P|_{\rm h} = (P|_{\rm h} + \epsilon|_{\rm h})\frac{\kappa v_{\rm c}^2}{1 - v_{\rm c}^2}, \qquad \frac{\epsilon}{\sigma}\bigg|_{\rm h} = \left(T|_{\rm h} + \frac{\mu_{\rm b}\nu_{\rm b}}{\sigma}\bigg|_{\rm h}\right)\left(1 + \frac{\kappa v_{\rm c}^2}{1 - v_{\rm c}^2}\right). \tag{4}$$

Using extensive variables we obtain [4]:

$$\frac{E}{S}\bigg|_{\rm h} = (T|_{\rm h} + \delta T|_{\rm h})\left(1 + \frac{\kappa v_{\rm c}^2}{1 - v_{\rm c}^2}\right), \quad \delta T = \mu_{\rm b}\frac{\nu_{\rm b}}{\sigma} = \frac{\mu_{\rm b}}{S/b}. \tag{5}$$

For RHIC, we have $\delta T|_{\rm h} < 0.4$ MeV, considering that $\mu_{\rm b} < 40$ MeV and

$S/b > 100$; at top SPS energy, we have $\mu_{\rm b} \simeq 200$–250 MeV and $S/b \simeq 25$–45, and thus, $\delta T|_{\rm h} \simeq 5$ MeV.

The usefulness of Eq. (5) comes from the observation that it implies:
$$\left. \frac{E}{S} \right|_{\rm h} > T|_{\rm h} \,. \tag{6}$$
This is a near equality since the geometric emissivity factor κ is positive and small, especially so at RHIC, and $v_{\rm c}^2 < 1/3$.

The Gibbs–Duham relation also implies: $E/S + PV/S = T + \delta T > T$. One would think that the PV term is small, since the pressure is small as the lattice calculations suggest, $\epsilon/P \to 7$. However, this in principle can be compensated by large volume of hadronization. Since the volume is a directly measured quantity, this hadronization requirement can not remain unnoticed for long. In fact, the HBT results today place a very severe constraint on the emitter size of the pion source. With realistic volume size, the PV term is negligible. In this case, we obtain just as in Eq. (6), $E/S \simeq T$.

In Eq. (6), we have thus a necessary statistical hadronization constraint. In our experience, this is practically impossible to accomplish in chemical equilibrium statistical hadronization models. The reason is that, in such an approach, a rather high temperature $T \simeq 175$ MeV is required to accommodate the high intrinsic entropy content of hadron source, but this does not drive up sufficiently the energy content, since for pions in equilibrium $E/S < T$. What happens in such an approach is that a very large hadronization volume is required, in disagreement with the HBT results. We conclude that the combination of HBT result with fundamental properties of statistical physics requires chemical non-equilibrium statistical hadronization.

3 Hadron Phase Space

We consider a generalization of Fermi's statistical model of hadron production [5,6], and consider the yield of hadrons to be solely dictated by the study of the magnitude of the phase space available.

The relative number of final state hadronic particles freezing out from, e.g., a thermal quark–gluon source, is obtained noting that the fugacity f_i of the i-th emitted composite hadronic particle containing k-components is derived from fugacities λ_k and phase space occupancies γ_k:
$$N_i \propto e^{-E_i/T_{\rm f}} f_i = e^{-E_i/T_{\rm f}} \prod_{k \in i} \gamma_k \lambda_k. \tag{7}$$
In most cases, we study chemical properties of light quarks u, d jointly, though on occasion, we will introduce the isospin asymmetry. As seen in Eq. (7), we study particle production in terms of five statistical parameters

$T, \lambda_{\mathrm{q}}, \lambda_{\mathrm{s}}, \gamma_{\mathrm{q}}, \gamma_{\mathrm{s}}$. In addition, to describe the shape of spectra, one needs matter flow velocity parameters, these become irrelevant when only total particle abundances are studied, obtained integrating all of phase space, or equivalently in presence of strong longitudinal flow, when we are looking at a yield per unit of rapidity.

The difference between the two types of chemical parameters, λ_i and γ_i, is that the phase space occupancy factor γ_i regulates the number of pairs of flavor 'i', and hence applies in the same manner to particles and antiparticles, while fugacity λ_i applies only to particles, while λ_i^{-1} is the antiparticle fugacity.

The resulting yields of final state hadronic particles are most conveniently characterized taking the Laplace transform of the accessible phase space. This approach generates a function which, in its mathematical properties, is identical to the partition function:

$$\mathcal{L}\left[e^{-E_i/T_{\mathrm{f}}}\prod_{k\in i}\gamma_k\lambda_k\right]\propto\ln\mathcal{Z}^{\mathrm{HG}}\,.\tag{8}$$

Eq. (8) does not require formation of a phase comprising a gas of hadrons, but is not inconsistent with such a step in evolution of the matter; it describes not a partition function, but just a look-alike object arising from the Laplace transform of the accessible phase space. The final particle abundances, measured in an experiment, are obtained after all unstable hadronic resonances 'j' are allowed to disintegrate, contributing to the yields of stable hadrons.

The unnormalized particle multiplicities are obtained differentiating Eq. (8) with respect to particle fugacity. The relative particle yields are simply given by ratios of corresponding chemical factors, weighted with the size of the momentum phase space accepted by the experiment. The ratios of strange antibaryons to strange baryons *of same particle type* are, in our approach, simple functions of the quark fugacities.

4   Strange Hadrons at SPS

We expect, in sudden hadronization, chemical non-equilibrium at hadron freeze-out. Full chemical non-equilibrium description of particle yields is required to arrive at a statistically significant description of the data with small error:

$$\chi^2\equiv\frac{\sum_j(R_{\mathrm{th}}^j-R_{\mathrm{exp}}^j)^2}{(\Delta R_{\mathrm{exp}}^j)^2}\,.\tag{9}$$

It is common to normalize the total error χ^2 by the difference between the number of data points and parameters used, the so called 'dof' (degrees of freedom) quantity. For systems we study, with a few degrees of freedom

Table 1. WA97 (top) and NA49 (bottom) Pb–Pb 158A GeV collision hadron ratios compared with phase space fits.

Ratios	Ref.	Exp. Data	Pb$\vert^{\mathrm{s},\gamma_{\mathrm{q}}}$	Pb$\vert^{\gamma_{\mathrm{q}}}$
Ξ/Λ	[7]	0.099 ± 0.008	0.096	0.095
$\overline{\Xi}/\bar{\Lambda}$	[7]	0.203 ± 0.024	0.197	0.199
$\bar{\Lambda}/\Lambda$	[7]	0.124 ± 0.013	0.123	0.122
$\overline{\Xi}/\Xi$	[7]	0.255 ± 0.025	0.251	0.255
$\mathrm{K}^+/\mathrm{K}^-$	[8]	1.80 ± 0.10	1.746	1.771
K^-/π^-	[9]	0.082 ± 0.012	0.082	0.080
$\mathrm{K}^0_{\mathrm{s}}/b$	[10]	0.183 ± 0.027	0.192	0.195
h^-/b	[11]	1.97 ± 0.1	1.786	1.818
ϕ/K^-	[12]	0.145 ± 0.024	0.164	0.163
$\bar{\Lambda}/\bar{\mathrm{p}}$	$y = 0$		0.565	0.568
$\bar{\mathrm{p}}/\pi^-$	all y		0.017	0.016
	χ^2		1.6	1.15
	$N;p;r$		9;4;1	9;5;1

(typically 5–15), a statistically significant fit requires that $\chi^2/\mathrm{dof} < 1$. For just a few 'dof', the error should be as small as $\chi^2/\mathrm{dof}< 0.5$. The usual requirement $\chi^2 \to 1$ is only applying for very large 'dof'.

Turning to the Pb–Pb system at 158A GeV collision energy, we consider particle listed in table 1, top section from the experiment WA97, for $p_\perp > 0.7\,$GeV, within a narrow $\Delta y = 0.5$ central rapidity window. Further below are shown results from the large acceptance experiment NA49, extrapolated by the collaboration to full 4π phase space coverage. The total error χ^2 for the two result columns is shown at the bottom of this table along with the number of data points 'N', parameters 'p' used, and number of (algebraic) redundancies 'r' connecting the experimental results. For $r \neq 0$, it is more appropriate to quote the total χ^2, since the statistical relevance condition is more difficult to establish given the constraints, but since $\chi^2/(N-p-r) < 0.5$, we are certain to have a valid description of hadron multiplicities.

In second last column, the superscript 's' means that λ_{s} is fixed by strangeness balance and, superscript 'γ_{q}', in two last columns, means that $\gamma_{\mathrm{q}} = \gamma_{\mathrm{q}}^{\mathrm{c}} = e^{m_\pi/2T_{\mathrm{f}}}$, is fixed to maximize the entropy content in the hadronic phase space. The fits presented are obtained with latest NA49 experimental results, i.e., have updated h^-/b, newly published ϕ yield [11], and we predict the $\bar{\Lambda}/\bar{\mathrm{p}}$ ratio. b is here the number of baryon participants, and $h^- = \pi^- + \mathrm{K}^- + \bar{\mathrm{p}}$

Table 2. Upper section: statistical model parameters which best describe the experimental results for Pb–Pb data seen in Fig. 1. Bottom section: energy per entropy, antistrangeness, net strangeness of the full hadron phase space characterized by these statistical parameters. In column two, we fix λ_s by requirement of strangeness conservation, and in this and next column we fix $\gamma_q = \gamma_q^c$. Superscript * indicates values which are result of a constraint.

	$\text{Pb}\vert_v^{s,\gamma_q}$	$\text{Pb}\vert_v^{\gamma_q}$
T [MeV]	151 ± 3	147.7 ± 5.6
v_c	0.55 ± 0.05	0.52 ± 0.29
λ_q	1.617 ± 0.028	1.624 ± 0.029
λ_s	1.10^*	1.094 ± 0.02
γ_q	$\gamma_q^{c*} = e^{m_\pi/2T_f} = 1.6$	$\gamma_q^{c*} = e^{m_\pi/2T_f} = 1.6$
γ_s/γ_q	1.00 ± 0.06	1.00 ± 0.06
E/b[GeV]	4.0	4.1
s/b	0.70 ± 0.05	0.71 ± 0.05
E/S[MeV]	163 ± 1	160 ± 1
$(\bar{s} - s)/b$	0^*	0.04 ± 0.05

is the yield of stable negative hadrons which includes pions, kaons and antiprotons. We see, comparing the two columns, that strangeness conservation (enforced in second last column) is consistent with the experimental data shown, enforcing it does not change much the results for particle multiplicities.

The six parameters $(T, v_c, \lambda_q, \lambda_s, \gamma_q, \gamma_s)$ describing the particle abundances are shown in the top section of table 2. Since the results of the WA97 experiment are not covering the full phase space, there is a reasonably precise value found for one velocity parameter, taken to be the spherical surface flow velocity v_c of the fireball hadron source.

A value $\lambda_s^{\text{Pb}} \simeq 1.1$ characteristic for a source of freely movable strange quarks with balancing strangeness in presence of strong Coulomb potential [13], i.e., with $\tilde{\lambda}_s = 1$, is obtained. Since all chemical non equilibrium studies of the Pb–Pb system converge to the case of maximum entropy, we have presented the results with fixed $\gamma_q = \gamma_q^c = e^{m_\pi/2T_f}$. The large values of $\gamma_q > 1$ confirm the need to hadronize the excess entropy of the QGP possibly formed. This value is derived from both the specific negative hadron h^-/b abundance and from the relative strange hadron yields.

The fits shown satisfy comfortably the statistical hadronization constraint that $E/S > T$ discussed in section 2. We see also that near strangeness balance is obtained as result of the fit.

One of the interesting quantitative results of this analysis is shown in the bottom section of table 2: the yield of strangeness per baryon, $s/b \simeq 0.7$. As we will show in Fig. 1, the expected equilibrium yield is $s/b|^{\mathrm{QGP}} \simeq 1.4$, and thus we have $\gamma_{\mathrm{s}}^{\mathrm{QGP}} \simeq 0.5$ at SPS. Since the occupancy values in table 2 are derived from hadron phase space, we thus find $\gamma_{\mathrm{s}}^{\mathrm{HG}}/\gamma_{\mathrm{s}}^{\mathrm{QGP}} \simeq 3$.

5 Strangeness at RHIC

In the likely event that the QGP formed at RHIC evolves towards strangeness chemical equilibrium abundance, or possibly even exceeds it, we should expect a noticeable over occupancy of strangeness as measured in terms of chemical equilibrium final state hadron abundance. Because much of the strangeness is in the baryonic degrees of freedom, the kaon to pion ratio should appear suppressed, compared to SPS results. An even more penetrating effect of the hadronization of strangeness rich QGP at RHIC is the abundant formation of strange baryons and antibaryons [14]. This high phase space occupancy is one of the requirements for the enhancement of multistrange (anti)baryon production, which is an important hadronic signal of QGP phenomena [15]. In particular, we hope that hadrons produced in phase space with a small probability, such as Ω, $\overline{\Omega}$, will be observed with a yield above statistical hadronization expectations, continuing the trend seen at SPS.

The RHIC data we consider are were obtained in $\sqrt{s_{\mathrm{NN}}} = 130$ GeV run at the central rapidity region where, due to approximate longitudinal scaling, the effects of flow cancel and we can evaluate the full phase space yields in order to obtain particle ratios. We do not fit trivial results such as $\pi^+/\pi^- = 1$, since the large hadron yield combined with the flow of baryon isospin asymmetry towards the fragmentation rapidity region assures us that this result will occur to a great precision. We also do not use the results for $\mathrm{K}^*, \bar{\mathrm{K}}^*$ since these yields depend on the degree of rescattering of resonance decay products. The data we consider has been reported by the STAR collaboration of Summer 2001, and where available is combined with data of PHENIX, BRAHMS, PHOBOS, for more discussion of the data origin, see [16]. We assume, in our fit in table 3, that the multistrange weak interaction cascading $\Xi \to \Lambda$, in the STAR result we consider, is cut by vertex discrimination and thus we use these yields without a further correction.

We first consider what experimental hadron yield results shown in table 3 imply about total strangeness yield in the RHIC-130 fireball. We begin with the yield of strange quarks contained in hyperons. We have, in singly strange hyperons, 1.5 times the yield observed in Λ, since $\Sigma^\pm$ remain unobserved. Also, accounting for the doubly strange Ξ^- which are half of the all Ξ, and

contain two strange quarks, we have:

$$\frac{\langle s \rangle_{\mathrm{Y}}}{\mathrm{h}^-} = 1.5 \cdot 0.059 + 2 \cdot 2 \cdot 0.195 \cdot 0.059 = 0.133 \,.$$

Allowing for the unobserved Ω at the theoretical rate, this number increases to $\langle s \rangle_{\mathrm{Y}}/\mathrm{h}^- = 0.14$. Repeating the same argument for antihyperons the result is 0.10. s and $\bar{\mathrm{s}}$ content in kaons is four times that in $\mathrm{K_S}$ and thus the total strangeness yield is

$$\frac{\langle \mathrm{s} + \bar{\mathrm{s}} \rangle}{\mathrm{h}^-} = 0.76 \,,$$

with 32% of this yield contained in hyperons and antihyperons. This amounts to about 1.5 fold enhancement compared to highest SPS energies, with (multi)strange hyperons and antihyperons being a very important component.

We now discuss the fits of RHIC-130 results. In the last column in table 3, the chemical equilibrium fit, the large χ^2 originates in the inability to account for multistrange $\overline{\Xi}$, Ξ. Similar results are presented in Ref. [16], which work does not include multistrange hadrons. This equilibrium fit yields $E/S = 159\,\mathrm{MeV} < T = 183\,\mathrm{MeV}$ contradicting the conditions we discussed in depth in section 2. On the other hand, the chemical nonequilibrium fits come out to be in near perfect agreement with data, and consistent with the QGP statistical hadronization picture: $E/S = 163 > T = 158\,\mathrm{MeV}$ and $\gamma_{\mathrm{s}}, \gamma_{\mathrm{q}} > 1$. The value of the hadronization temperature $T = 158\,\mathrm{MeV}$ is below the central expected equilibrium phase transition temperature, and this hadronization temperatures at RHIC is consistent with sudden breakup of a supercooled QGP fireball. The inclusion of the yields of multistrange antibaryons in the RHIC data analysis, along with allowance for chemical non-equilibrium ($\gamma \neq 1$), allows to discriminate the different (chemical equilibrium/nonequilibrium) reaction scenarios.

The value of the thermal energy content $E/b = 25$ GeV, seen in table 3, is in very good agreement with expectations once we allow for the kinetic energy content associated with longitudinal and transverse motion. The energy of each particle is 'boosted' with the factor $\gamma_\perp^v \cosh y_\parallel$. For $v_\perp = c/\sqrt{3}$, we have $\gamma_\perp^v = 1.22$. The longitudinal flow range is about ± 2.3 rapidity units, according to PHOBOS results. To obtain the energy increase due to longitudinal flow, we have to multiply by the average, $\int dy_\parallel \cosh y_\parallel / y_\parallel \rightarrow \sinh(2.3)/2.3 = 2.15$, for a total average increase in energy by factor 2.62, which takes the full energy content to $E^v/b \simeq 65$ GeV as expected. This consistency reassures that we have a physically relevant fit of the data, which respects overall energy conservation.

We analyze next the strangeness content, $s/b = 6$, seen table 3. The fully equilibrated QGP phase space would have yielded 8.6 strange quark pairs per

Table 3. Fits of central rapidity hadron ratios for RHIC $\sqrt{s_{\mathrm{NN}}} = 130$ GeV run. Top section: experimental results, followed by chemical parameters, physical property of the phase space, and the fit error. Columns: data, full non-equilibrium fit, nonequilibrium fit constrained by strangeness conservation and supersaturation of pion phase space, and in the last column, equilibrium fit constrained by strangeness conservation, upper index * indicates quantities fixed by these considerations.

	Data	Fit	Fit $s - \bar{s} = 0$	Fit$^{\mathrm{eq}}$ $s - \bar{s} = 0$
$\bar{\mathrm{p}}/\mathrm{p}$	0.64 ±0.07	0.637	0.640	0.587
$\bar{\mathrm{p}}/\mathrm{h}^-$		0.068	0.068	0.075
$\overline{\Lambda}/\Lambda$	0.77 ±0.07	0.719	0.718	0.679
Λ/h^-	0.059±0.001	0.059	0.059	0.059
$\overline{\Lambda}/\mathrm{h}^-$	0.042±0.001	0.042	0.042	0.040
$\overline{\Xi}/\Xi$	0.83 ±0.08	0.817	0.813	0.790
Ξ^-/Λ	0.195±0.015	0.176	0.176	0.130
$\overline{\Xi^-}/\overline{\Lambda}$	0.210±0.015	0.200	0.200	0.152
$\mathrm{K}^-/\mathrm{K}^+$	0.88 ±0.05	0.896	0.900	0.891
K^-/π^-	0.149±0.020	0.152	0.152	0.145
$\mathrm{K_S}/\mathrm{h}^-$	0.130±0.001	0.130	0.130	0.124
Ω/Ξ^-		0.222	0.223	0.208
$\overline{\Omega}/\overline{\Xi^-}$		0.257	0.256	0.247
$\overline{\Omega}/\Omega$		0.943	0.934	0.935
T		158± 1	158± 1	183± 1
γ_{q}		1.55±0.01	1.58±0.08	1^*
λ_{q}		1.082±0.010	1.081±0.006	1.097±0.006
γ_{s}		2.09±0.03	2.1±0.1	1^*
λ_{s}		1.0097±0.015	1.0114^*	1.011^*
$E/b[\mathrm{GeV}]$		24.6	24.7	21
s/b		6.1	6.2	4.2
S/b		151	152	131
$E/S[\mathrm{MeV}]$		163	163	159
χ^2/dof		2.95/(10−5)	2.96/(10−4)	73/(10−2)

baryon at $\lambda_{\mathrm{q}} = 1.08$, as is shown in Fig. 1 below. Thus $\gamma_{\mathrm{s}}^{\mathrm{QGP}} = 6/8.6 \simeq 0.7$, which is greater than the value 0.5 we found for the SPS energy range. Using the fitted value $\gamma_{\mathrm{s}}^{\mathrm{HG}} = 2.1$, we find again, just like we found in case of SPS, $\gamma_{\mathrm{s}}^{\mathrm{HG}}/\gamma_{\mathrm{s}}^{\mathrm{QGP}} \simeq 3$. The fact that the strangeness phase space in QGP is not fully saturated is, on a second careful look, in qualitative agreement with kinetic strangeness theory predictions [14], adjusting our study to the observed
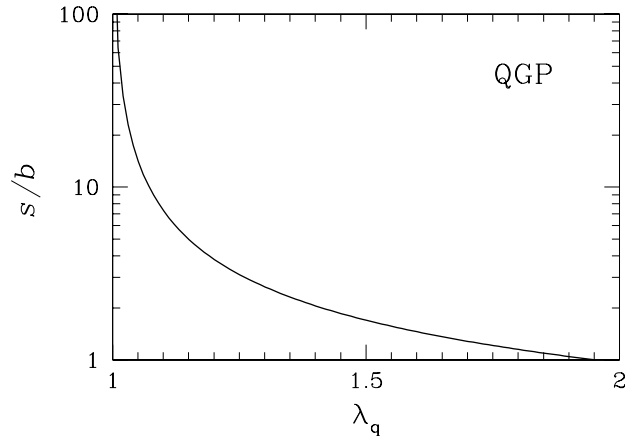
Figure 1. Strangeness yield per baryon as function of λ_q in equilibrated quark-gluon plasma.

RHIC-130 run conditions.

6 Strangeness as Signature of Deconfinement

We consider the ratio of equilibrium strangeness density, arising in the Boltzmann gas limit, to the baryon density in a QGP fireball. To first approximation, perturbative thermal QCD corrections cancel in the ratio. For $m_s = 200$ MeV and $T = 150$ MeV, we have:

$$\frac{s}{b} \simeq \gamma_s^{\rm QGP} \frac{0.7}{\ln \lambda_q + (\ln \lambda_q)^3/\pi^2} \ . \tag{10}$$

The relative yield s/b is mainly dependent on the value of λ_q, with only a slow temperature dependence contained in the coefficient 0.7 in Eq. (10). The light quark fugacity λ_q is usually independent of the strategy of data analysis, as is also seen in table 3.

At top SPS energy where $\lambda_q \simeq 1.6$, we see in Fig. 1 that the equilibrium strangeness yield is at 1.5 strange pairs per participating baryon. The actual experimental yield, 0.7, see table 2, is half as large as in an equilibrated QGP, but is 2.5 times the yield in p–p reactions. At the RHIC 130 GeV run, the value $\lambda_q = 1.08$, see table 3, and the specific strangeness yield in a QGP fireball at equilibrium is an order of magnitude greater than currently observed at SPS top energy. As discussed, the actual yield corresponds to 70% of the full phase space. A further increase towards equilibrium yield at higher RHIC-

200 energy range is expected. The remarkable feature of the RHIC situation is that much of strangeness enhancement is found in the (multistrange) baryon abundance. Given the large strangeness per baryon ratio, Fig. 1, baryons and antibaryons produced from QGP at RHIC have been predicted to be mostly strange [14].

The high specific strangeness yield s/b is a clear indicator for the extreme conditions reached in heavy ion collisions. An equally interesting observable is the occupancy of the strangeness phase space. In sudden hadronization, $V^{\mathrm{HG}}/V^{\mathrm{QGP}} \simeq 1$, the growth of volume is negligible, $T^{\mathrm{QGP}} \simeq T^{\mathrm{HG}}$, the temperature is maintained across the hadronization front, and the chemical occupancy factors in both states of matter accommodate the different magnitude of the particle phase space. In this case, the QGP strangeness when 'squeezed' into the smaller HG phase space results in $\gamma_{\mathrm{s}}^{\mathrm{HG}}/\gamma_{\mathrm{s}}^{\mathrm{QGP}} \simeq 3$, which is of the same magnitude as the unfrozen color degeneracy. This theoretical expectation is indeed observed both at top SPS and RHIC-130 run, as we have reported.

For the top SPS energy range this interesting result could be ignored, since accidentally $\gamma_{\mathrm{s}}^{\mathrm{HG}}/\gamma_{\mathrm{q}}^{\mathrm{HG}} \simeq 1$. Thus one can also model the hadronization at SPS energy in terms of an equilibrium hadronization model. The pion enhancement associated with the high entropy phase can be accommodated by use of two temperatures, one for the determination of absolute particle yields, and another for determination of the spectral shape. Such an approach has similar number of parameters, and comparable predictive power, the only inconsistency (with HBT) is the large volume required, as we have discussed. However, the condition, $\gamma_{\mathrm{s}}^{\mathrm{HG}}/\gamma_{\mathrm{q}}^{\mathrm{HG}} \simeq 1$, is not present at the RHIC energy range, where already at RHIC-130 the hadron phase space occupancy for strangeness is significantly larger than for light quarks, see table 3. It is the inclusion of the yields of multistrange antibaryons in the RHIC data analysis, which leads to this result.

We see, at SPS and at RHIC, considerable convergence of the hadron production around properties of suddenly hadronizing entropy and strangeness rich QGP. The QGP phase strangeness occupancy rises from $\gamma_{\mathrm{s}}^{\mathrm{QGP}} \simeq 0,5$ at SPS $\sqrt{s_{\mathrm{NN}}} = 17.2$ GeV, to $\gamma_{\mathrm{s}}^{\mathrm{QGP}} \simeq 0.7$ at $\sqrt{s_{\mathrm{NN}}} = 130$ GeV, and there is still space for a further strangeness yield rise at highest RHIC energy $\sqrt{s_{\mathrm{NN}}} = 200$ GeV. In conclusion: the deconfined thermal QGP phase manifests itself through its gluon content, which generates in thermal collision processes a clear strangeness fingerprint of QGP.

References

1. J. Rafelski and B. Müller, 1982. Strangeness production in the quark–gluon plasma. *Phys. Rev. Lett.*, **48**, 1066. See: *Phys. Rev. Lett.*, **56**, 2334E (1986).
2. F. Karsch, E. Laermann, and A. Peikert, 2000. The pressure in 2, 2+1 and 3 flavour QCD. *Phys. Lett.* B, **478**, 447.
3. S.A. Chin, 1978. Transition to hot quark matter in relativistic heavy-ion collision. *Phys. Lett.* B, **78**, 552.
4. J. Rafelski and J. Letessier, 2000. Sudden hadronization in relativistic nuclear collisions. *Phys. Rev. Lett.*, **85**, 4695.
5. E. Fermi, 1950. High-energy nuclear events. *Prog. Theo. Phys.*, **5**, 570.
6. E. Fermi, 1953. Multiple production of pions in nucleon–nucleon collisions at cosmotron energies. *Phys. Rev.*, **92**, 452.
7. I. Králik, *et al.*, WA97 collaboration, 1998. Λ, Ξ and Ω production in Pb–Pb collisions at $158A$ GeV. *Nucl. Phys.* A, **638**, 115.
8. C. Bormann, *et al.*, NA49 collaboration, 1997. Kaon, lambda and antilambda production in Pb+Pb collisions at 158 GeV per nucleon. *J. Phys.* G *Nucl. Part. Phys.*, **23**, 1817.
9. F. Siklér *et al.*, NA49 collaboration, 1999. Hadron production in nuclear collisions from the NA49 experiment at $158A$ GeV. *Nucl. Phys.* A, **661**, 45c.
10. P.G. Jones *et al.*, NA49 collaboration, 1996. Hadron yields and hadron spectra from the NA49 experiment. *Nucl. Phys.* A, **610**, 188c.
11. H. Appelshäuser *et al.*, NA49 collaboration, 1999. Baryon stopping and charged particle distributions in central Pb+Pb collisions at 158 GeV per nucleon. *Phys. Rev. Lett.*, **82**, 2471.
12. S.V. Afanasev *et al.*, NA49 collaboration, 2000. Production of ϕ mesons in p+p, p+Pb and central Pb+Pb collisions at $E_{\mathrm{beam}} = 158A$ GeV. *Phys. Lett.* B, **941**, 59.
13. J. Letessier and J. Rafelski, 1999. Diagnostics of QGP with strange hadrons. *Acta Phys. Pol.* B, **30**, 3559.
14. J. Rafelski and J. Letessier, 1999. Expected production of strange baryons and antibaryons in baryon-poor QGP. *Phys. Lett.* B, **469**, 12.
15. J. Rafelski, 1982. Formation and observables of the quark gluon plasma. *Phys. Rep.*, **88**, 331.
16. P. Braun-Munzinger, D. Magestro, K. Redlich, and J. Stachel, 2001. Hadron production in Au–Au collisions at RHIC. *Phys. Lett.* B, **518**, 41.